40th Fluid Dynamics Conference and Exhibit
28 June - 1 July 2010, Chicago, Illinois

AIAA 2010-5030

A High Order Conservative Upwind Algorithm for the Incompressible Navier Stokes Equations

Debojyoti Ghosh * and James D. Baeder †
University of Maryland, College Park, MD 20742, USA

The incompressible Navier Stokes equations are solved numerically using the Fractional Step algorithm. A Cartesian staggered-grid solver based on a high order upwind reconstruction of the convective flux is developed for high Reynolds number and inviscid flows. The Weighted Essentially Non-Oscillatory Schemes are used in conjunction with Runge-Kutta time-stepping. Upwinding based on velocity components is necessary for non-oscillatory and stable solutions at high Reynolds numbers. The conservative and non-conservative flux formulations are compared since differences are expected due to the numerical error in satisfying the continuity equation. The algorithm is validated against benchmark flow problems. The accuracy and convergence properties are analyzed on an isolated vortex convection problem. Finally, the performance of the algorithm on inviscid problems with strong gradients is demonstrated by simulating the evolution of a shear layer and leapfrogging of vortex rings.

I. Introduction

The Navier Stokes equations form the governing set of equations for fluid motion under the continuum assumption. At flow speeds which are much lower than the speed of sound in the medium, the density is assumed to be constant and the incompressible Navier Stokes equations[1,2] are used to obtain the flow field. In this paper a numerical method for solving these equations is presented with particular focus on obtaining solutions for high Reynolds number flows. Various formulations of the governing equations have been used,[2,3] which include the primitive variable formulation, the pressure-Poisson formulation, the vorticity formulation and the vorticity-streamfunction formulation. Each of these formulations is mathematically equivalent if physically relevant initial and boundary conditions satisfying mass continuity are specified. In the present study, the primitive variable formulation has been adopted for its relative simplicity. It provides a straightforward representation of the Navier Stokes equations and the implementation of boundary conditions on primitive variables is relatively intuitive.

The numerical methods for the primitive variable formulation can be classified into three broad categories. One of them is the family of schemes with implicit pressure correction[4,5] and these have been applied to steady or quasi-steady problems where time-accuracy is not required. Another family of numerical methods are the artificial compressibility methods[5,6,9] which cast the governing equations in a form similar to that of the compressible Navier-Stokes equations by introducing an artificial density variable. While this allows the application of numerical schemes developed for the compressible flow equations to the incompressible ones, it introduces an arbitrary parameter. Satisfaction of mass continuity renders the system of equations stiff for unsteady problems. The projection schemes or the fractional step schemes[7,8,10] have been reported to be the best suited for time-accurate computations of unsteady flows. These methods are based on the splitting of a vector field into its solenoidal and non-solenoidal components. A predicted velocity field is computed based on the convective and diffusive terms and a pressure-based correction is used to enforce the divergence-free condition of mass conservation. In the present study, the fractional step method is used because the algorithm is primarily intended for simulation of unsteady flows.

While the incompressible Navier Stokes equations do not admit discontinuous solutions, steep gradients may develop in flows with strong shear layers and concentrated vortices. In the low Reynolds number

*Graduate Research Assistant, Applied Mathematics & Statistics, and Scientific Computation, ghosh@umd.edu.
†Associate Professor, Department of Aerospace Engineering and Associate Fellow, AIAA, baeder@umd.edu.

regime, central differencing of spatial derivatives is sufficient to give satisfactory results[10] because the viscosity present in the system dampens the oscillatory behavior of central schemes. At higher Reynolds number, upwinding is required to prevent spurious oscillations. A primitive variable algorithm based on an upwind flux reconstruction and Weighted Essentially Non-Oscillatory (WENO) interpolation has recently been presented.[11] It uses a non-conservative form of the convective terms and discretizes them in an upwind fashion. In the present study, a Cartesian staggered-grid fractional step solver using upwind spatial reconstruction is presented that uses the conservative form of the convective terms. The two formulations are mathematically identical under the condition that the incompressible continuity equation is exactly satisfied. However, in the numerical solutions, there is a finite non-zero divergence present in the computed solution and thus, differences are expected between solutions resulting from using the conservative and non-conservative formulations. An effort is made to study and document these differences for inviscid problems. Overall, the aim is to develop a high order accurate algorithm for the incompressible equations which can solve high Reynolds number and inviscid flows.

II. Methodology

II.A. Governing Equations

The governing equations for incompressible flows are obtained from the generalized Navier-Stokes equations by assuming the density to be constant. This results in the expression for the conservation of mass as

$$\frac{\partial u_i}{\partial x_i} = 0 \tag{1}$$

where u_i is the component of the velocity vector along x_i. The momentum equations can be expressed as

$$\frac{\partial u_i}{\partial t} + \frac{\partial (u_i u_j)}{\partial x_j} = -\frac{\partial p}{\partial x_i} + \nu \frac{\partial^2 u_i}{\partial x_j \partial x_j} \tag{2}$$

where p is the pressure and ν is the coefficient of viscosity. The energy equation is decoupled from the system and is not solved as a part of the main solution algorithm. Using the conservation of mass equation, the momentum equations can also be written as

$$\frac{\partial u_i}{\partial t} + u_j \frac{\partial u_i}{\partial x_j} = -\frac{\partial p}{\partial x_i} + \nu \frac{\partial^2 u_i}{\partial x_j \partial x_j} \tag{3}$$

Equation (2) uses a conservative form of the convective terms while Eq. (3) uses a non-conservative form. They are identical if Eq. (1) is exactly satisfied.

II.B. Numerical Method

The Fractional Step algorithm[10] is used to integrate the governing equations in time. The predictor step involves the calculation of a velocity field $\mathbf{u}^*$ based on the convective and diffusive terms in Eqs. (2) and (3). The corrector step is then used to compute a pressure field consistent with the continuity equation given by Eq. (1). The predicted velocity $\mathbf{u}^*$ is then corrected to ensure that the solution at the next time step is divergence free.

To prevent the pressure-velocity decoupling seen in collocated variable algorithms, the equations are discretized and solved on a staggered mesh. If (i, j, k) are the mesh indices corresponding to (x, y, z) axes respectively, then u (x-velocity) is stored at $(i + 1/2, j, k)$, v (y-velocity) is stored at $(i, j + 1/2, k)$ and w (z-velocity) is stored at $(i, j, k + 1/2)$.

The momentum equations excluding the pressure terms are solved in the predictor step. For the conservative form given by Eq. (2), the predictor step computes the solution of the following system of equations,

$$\begin{bmatrix} u \\ v \\ w \end{bmatrix}_t + \begin{bmatrix} u^2 \\ uv \\ uw \end{bmatrix}_x + \begin{bmatrix} uv \\ v^2 \\ vw \end{bmatrix}_y + \begin{bmatrix} uw \\ vw \\ w^2 \end{bmatrix}_z = \nu \begin{bmatrix} u_{xx} + u_{yy} + u_{zz} \\ v_{xx} + v_{yy} + v_{zz} \\ w_{xx} + w_{yy} + w_{zz} \end{bmatrix} \tag{4}$$

The corresponding system for the non-conservative form given by Eq. (3) can be written as,

$$\begin{bmatrix} u \\ v \\ w \end{bmatrix}_t + u \begin{bmatrix} u \\ v \\ w \end{bmatrix}_x + v \begin{bmatrix} u \\ v \\ w \end{bmatrix}_y + w \begin{bmatrix} u \\ v \\ w \end{bmatrix}_z = \nu \begin{bmatrix} u_{xx} + u_{yy} + u_{zz} \\ v_{xx} + v_{yy} + v_{zz} \\ w_{xx} + w_{yy} + w_{zz} \end{bmatrix} \tag{5}$$

Time integration of the convective terms is carried out using either the second order Adams-Bashforth (AB2) scheme or the Low-Storage third order Runge-Kutta (RK3) scheme. The viscous terms are treated using the trapezoidal scheme to remove the restrictive time-step size limit. It should be noted that for higher Reynolds number flows, the diffusion number is considerably low and explicit treatment of the viscous terms suffices.

The convective terms in the conservative flux formulation have the general form given by the second term on the left hand side of Eq. (2) which are discretized using a conservative discretization. As an example, the discretization of the y-component of the flux in the x-momentum equation is

$$\frac{\partial (uv)}{\partial y} \approx \frac{(uv)_{i+1/2,j+1/2,k} - (uv)_{i+1/2,j-1/2,k}}{y_{j+1/2} - y_{j-1/2}} \tag{6}$$

Note that in the staggered arrangement, the control volume of the discretized x-momentum equation is centered at $(i + 1/2, j, k)$. The above expression requires the interpolated values of u and v at $(i + 1/2, j + 1/2, k)$ and $(i + 1/2, j - 1/2, k)$. Using second order central differences, these values can be obtained by averaging the two neighboring values.

$$u_{i+1/2,j+1/2,k} = \frac{1}{2}(u_{i+1/2,j,k} + u_{i+1/2,j+1,k})$$
$$v_{i+1/2,j+1/2,k} = \frac{1}{2}(v_{i,j+1/2,k} + v_{i+1,j+1/2,k})$$

In an upwind reconstruction for a given face, only the tangential velocity component is evaluated using a biased interpolation based on the sign of the normal velocity component. The velocity component normal to the face is computed using a centered stencil as upwinding it based on the sign of the tangential component would be non-physical. Thus, for the above example, u is computed at the face using a stencil centered around $u_{i+1/2,j,k}$ or $u_{i+1/2,j+1,k}$, depending on the signs of $v_{i,j+1/2,k}$ and $v_{i+1,j+1/2,k}$. The interpolated value of v at the face is computed using a centered stencil. If a n-th order biased stencil is used to compute the upwinded velocity component, a $(n-1)$-th order centered interpolation is used to compute the other component.

The general form of the convective flux terms in the non-conservative formulation is given by the second term on the left hand side of Eq. (3). The second order central scheme is equivalent to simple averaging. For an upwind scheme, the velocity component inside the derivative is upwinded based on the sign of the velocity component outside the derivative.[11] The discretization of the y-component of the flux in the x-momentum equation is considered. The discretized form of this term is

$$v \frac{\partial u}{\partial y} \approx v_{i+1/2,j,k} \frac{u_{i+1/2,j+1/2,k} - u_{i+1/2,j-1/2,k}}{y_{j+1/2} - y_{j-1/2}} \tag{7}$$

Thus, u is interpolated at $(i+1/2, j+1/2, k)$ using a stencil centered at $(i+1/2, j, k)$ or $(i+1/2, j+1, k)$ based of the signs of $v_{i,j+1/2,k}$ and $v_{i+1,j+1/2,k}$. It should be noted that the value of v is required at $(i + 1/2, j, k)$ and is computed using a centered 2D stencil spread of the appropriate order. A $(n-1)$-th order centered interpolation is used for the non-upwind component if a n-th order interpolation is used for the upwind component.

The upwinded velocity components are evaluated using a high order interpolation for the flux formulations. In the present study, third and fifth order interpolations with and without WENO limiting[12] are implemented. The spatial derivatives in the viscous terms are approximated using second order central differencing. Along with the trapezoidal scheme in time, they form a system of equations which is solved using the Strongly Implicit Procedure (SIP).[13] The system is diagonally dominant and converges (residual drop to machine zero) within a few sub-iterations. Thus, implicit treatment of the viscous terms does not substantially increase the time of computation and is retained even for higher Reynolds number cases.

The predicted velocity field $\mathbf{u}^*$ may have a non-zero divergence which needs to be corrected to satisfy mass conservation. Considering the pressure gradient terms which were omitted from Eqs. (4) and (5) and discretizing in time, the corrector step is expressed as

$$\frac{\mathbf{u}^{n+1} - \mathbf{u}^*}{\Delta t} = -\nabla\phi \tag{8}$$

where ϕ is the solution of the Poisson equation given by

$$\nabla^2\phi = \frac{1}{\Delta t}\nabla.\mathbf{u}^* \tag{9}$$

It should be noted that ϕ is a mathematical variable used to enforce mass continuity and is not the physical pressure.[3,10] In the staggered mesh arrangement, it is stored at (i, j, k) locations. Second order central differences are used for all derivatives in the above two equations. This results in a system of equations which is solved iteratively using the SIP. The system is not as diagonally dominant as the one in the predictor step and thus requires more sub-iterations for the residual to fall few orders of magnitude. Eq. (8) is used to obtain the velocity at the next time level.

II.C. Boundary Conditions

Boundary conditions are implemented using ghost points outside the domain. At far-field boundaries, the velocity at the ghost points is set to its freestream value while the time derivative is set to zero.

$$\begin{aligned} \mathbf{u}_{ghost} &= \mathbf{u}_{freestream} \\ \Delta\mathbf{u}_{ghost} &= 0 \end{aligned} \tag{10}$$

Solid boundaries are enforced by setting the velocity at the ghost points to zero. The normal gradient of the pseudo-pressure is set to zero at all boundaries.[3] This has been enforced with both first and second order biased (into the domain) difference approximations for the first derivative and there is significant improvement in results using the second order differencing.

III. Results

The present algorithm is validated for several problems and representative results are presented here. The first problem considered in this paper is the lid driven square cavity. It is chosen since it is a benchmark case for the validation of incompressible Navier Stokes solvers. To analyze the performance of the various schemes and the effect of using the different flux formulations discussed above, the convection of an isolated vortex is studied and the results are presented. The upwind schemes developed are primarily intended to provide a robust algorithm to handle steep gradients and this is validated using the double shear layer problem. Two three-dimensional cases pertaining to the convection and interaction of vortex rings are studied. The viscous interaction of two coplanar vortex rings is studied and compared with existing results for validation. In addition, the performance of the solver is demonstrated on the inviscid leapfrogging of two coaxial vortex rings.

III.A. Lid Driven Square Cavity

This test problem deals with the flow inside a square cavity with uniform horizontal flow or a moving lid covering the cavity. The flow is characterized by a primary vortex and up to three secondary vortices depending on the Reynolds number. Several computational solutions are available for this problem in literature, thus making this a benchmark problem. The domain is a unit square ($[0, 1] \times [0, 1]$). The initial condition consists of a clockwise rotating vortex given by

$$\begin{aligned} u &= y - 0.5 \\ v &= -(x - 0.5) \end{aligned}$$

Solid boundary conditions are imposed on the bottom, left and right boundaries while a unit horizontal velocity $u = 1,\ v = 0$ is imposed on the top boundary. A zero normal gradient is imposed for pressure on all

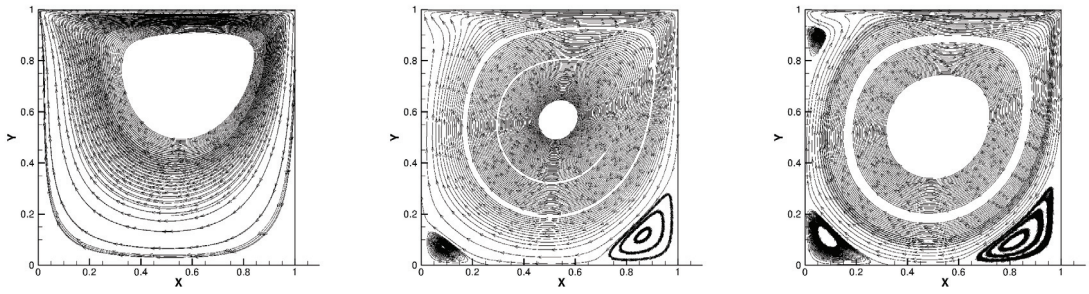

(a) Re 100 (b) Re 1000 (c) Re 3200

Figure 1. Streamlines for Lid Driven Square Cavity

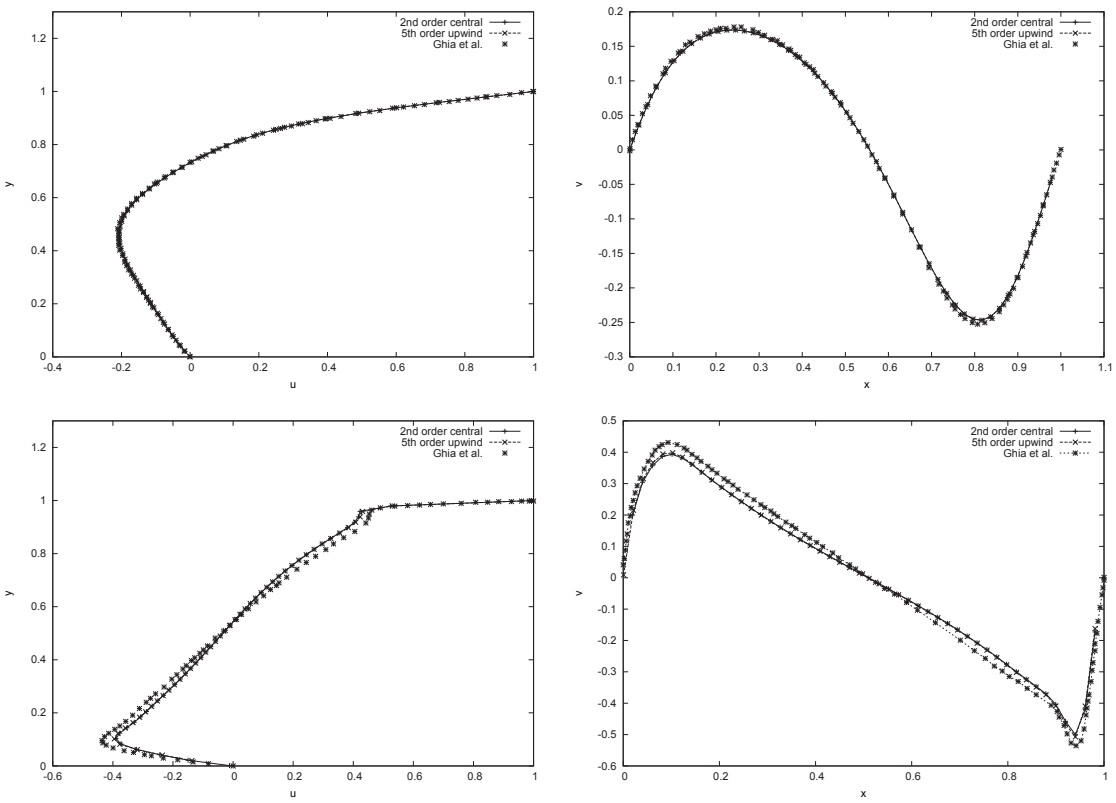

Figure 2. Cross-sectional Velocity Profiles for Reynolds numbers 100 and 3200

boundaries. The solution is marched in time till it reaches a steady state (i.e, the separation and attachment points of the secondary vortices become fixed).

Figure 1 shows the streamlines of the flow at three different Reynolds numbers. At a Reynolds number of 100, only the primary vortex is present. At a higher Reynolds number of 1000, the two secondary vortices form and at a still higher Reynolds number of 3200, a tertiary vortex is observed. These are consistent with what is reported in literature.[14]

Figure 2 shows the horizontal and vertical velocity profiles through the center of the domain for Reynolds numbers of 100 and 3200. All computations are carried out on a 130×130 grid.The results obtained using the second order central scheme and fifth order upwind scheme are compared with those reported.[14] AB2 time-stepping is used with second order reconstruction of the convective terms while RK3 time-stepping is used for fifth order spatial reconstruction. A good agreement is observed between the present results and the accepted ones. It can also be observed that in this case, where Reynolds numbers are relatively low, the second order central solutions and the fifth order upwind solutions are identical.

III.B. Taylor Vortex Convection

The convection of an isolated vortex is studied in this problem. The Taylor vortex is an exact solution of the Navier Stokes equations and its analytical form is given as[16]

$$u = \frac{-(y-y_c)}{1+2t/Re}\exp[\frac{1}{2}(1-\frac{(x-x_c)^2+(y-y_c)^2}{1+2t/Re})]+U$$
$$v = \frac{(x-x_c)}{1+2t/Re}\exp[\frac{1}{2}(1-\frac{(x-x_c)^2+(y-y_c)^2}{1+2t/Re})]$$

The Reynolds number is defined as $Re = u_{\theta 0} r_0/\nu$ ($u_{\theta 0}$ is the maximum azimuthal velocity at time $t = 0$ and r_0 is the initial radius of the vortex). The domain is $[-8, 8] \times [-8, 8]$ and the convection velocity is $U = 8$. Thus, with periodic boundary conditions, the time period is 2. The vortex is initially located at the center of the domain ($x_c = y_c = 0$ at $t = 0$).

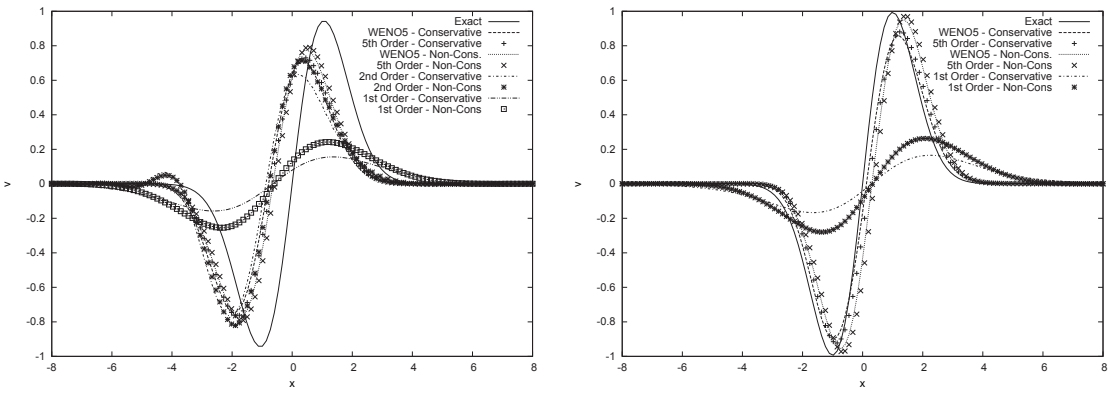

(a) Reynolds number 100 (b) Inviscid

Figure 3. Vortex Convection

The inviscid and viscous convection of the vortex is studied. The conservative and non-conservative flux formulations are both applied to this problem for second order central, fifth order upwind and fifth order upwind WENO interpolations. Time integration for the convective terms is carried out using the RK3 scheme. Viscous convection of the vortex is studied at a Reynolds number of 100. Figure 3(a) shows the v-velocity profile through the vortex core after three passes over the periodic domain on a 128×128 grid. The solutions for each pass are obtained at integer multiples of the time period ($t = 2, 4, 6$). It is observed that for second and fifth order interpolations, there is not much difference between using the conservative and non-conservative flux formulations. However, the 1st order results (with Euler Explicit time integration of convective terms) show that the non-conservative flux formulation is significantly less dissipative. An error in the convection speed is observed for all the schemes. It should be noted that even at a relatively low Reynolds number, the second order solution shows oscillations downstream of the vortex which are absent in the upwind fifth order solutions, with or without WENO limiting.

Figure 3(b) shows the v-velocity profile of the convecting vortex for the inviscid case (after three passes over the domain). Results are not shown for second order central interpolation since they are too oscillatory to yield a meaningful solution. The fifth order upwind schemes, with and without WENO limiting, are compared for both the conservative and non-conservative flux formulations. The schemes using the non-conservative flux formulation are observed to be less dissipative than the conservative ones. However, they contain a larger error in the convection speed of the vortex. The solution for this problem is smooth and there is only slight difference between fifth order upwind schemes with and without WENO limiting.

Successive grid refinement is used to assess the order of convergence for the various schemes. Errors are shown for third and fifth order WENO with conservative flux formulation (WENO3 and WENO5), the same with non-conservative flux formulation (WENO3-NC and WENO5-NC), third and fifth order interpolation with conservative (3rd Order and 5th Order) and non-conservative (3rd Order - NC and 5th Order - NC) flux formulations. The inviscid convection of the vortex is considered. Figure 4(a) shows the L_2 norm of the error in the u-velocity after one pass over the domain. The grid is refined from 40×40 to 320×320 and the results are obtained at a CFL number of 0.5. Figure 4(b) shows the same for the v-velocities. The

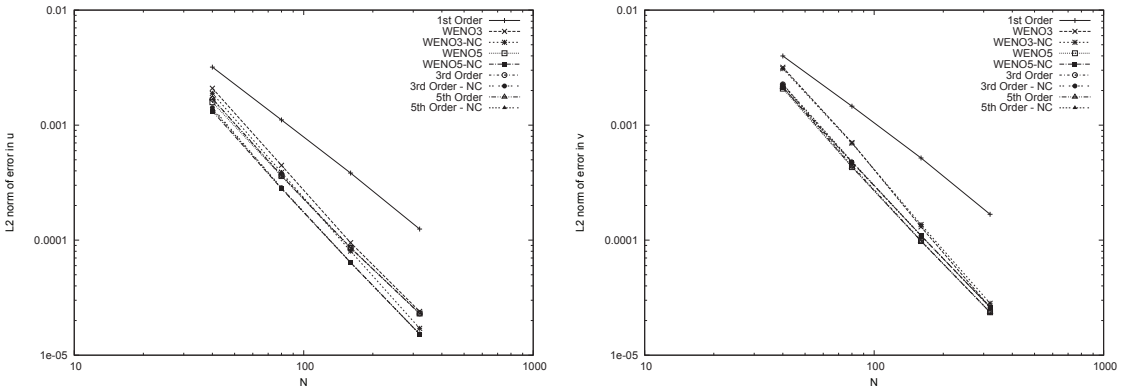

Figure 4. Convergence of Various Schemes for Vortex Convection Problem

higher order schemes achieve a convergence rate of around $O(N^{-2})$, which is less than the formal order of accuracy of the interpolations used in flux reconstruction. While the third and fifth order WENO schemes show similar orders of convergence, the absolute errors are less for higher order interpolation. The differences in the errors seem to be negligible between the third and fifth order schemes without WENO limiting. The Poisson solution in the corrector step is solved using second order spatial differencing and this could be the limiting factor. The conservative and non-conservative schemes have similar orders of convergence, though the non-conservative flux formulation results in lower absolute errors for this problem. This would indicate that the accuracy of the Poisson solver in the corrector step is decisive to the overall algorithm since the difference between the two formulations is the numerical error in satisfying mass conservation.

III.C. Double Shear Layer Test

The double shear layer test is a standard benchmark case for an inviscid, incompressible flow solver.[11,15] The initial flow consists of two shear layers with finite but small thickness. In the present study, the "thick" version of the shear layer test is solved since it is more suitable for validation. The velocity field is given as[15]

$$\begin{aligned} u(x,y) &= \tanh(\frac{1}{\rho}(y-\frac{\pi}{2})), \quad y < \pi \\ &= \tanh(\frac{1}{\rho}(\frac{3\pi}{2}-y)), \quad y \geq \pi \\ v(x,y) &= \delta \sin(x) \end{aligned}$$

In the present case, the value of the thickness parameter ρ is taken as $\pi/15$. The perturbation parameter for the v-velocity component δ is taken as 0.05. The domain is square of length 2π and periodic boundary conditions are applied on all boundaries. The evolution of the flow field is studied till a final time of $t = 14$. Figure 5 shows the evolution of the flow computed on a 256×256 grid using fifth order WENO interpolation with the conservative flux formulation and RK3 time stepping. The results agree well with those in literature.[11,15]

The different schemes are compared for this problem on a 128×128 grid. The second order central scheme yields extremely oscillatory results, thus reiterating that upwinding is required to obtain a non-oscillatory solution in the inviscid limit. The fifth order schemes yielded similar results with and without WENO limiting, despite this problem having very steep gradients. However, further tests need to be carried out for more complicated problems to determine if WENO limiting is necessary or if upwinding the flux provides sufficient stability.

III.D. Coplanar Vortex Ring Interaction

A 3D problem involving the collision of two vortex rings in space is used to validate the algorithm for viscous vortex interactions. Vortex interactions of this nature have been extensively studied[17] and can thus be used as a benchmark case. The initial flow consists of two vortex rings, each with a Gaussian azimuthal vorticity

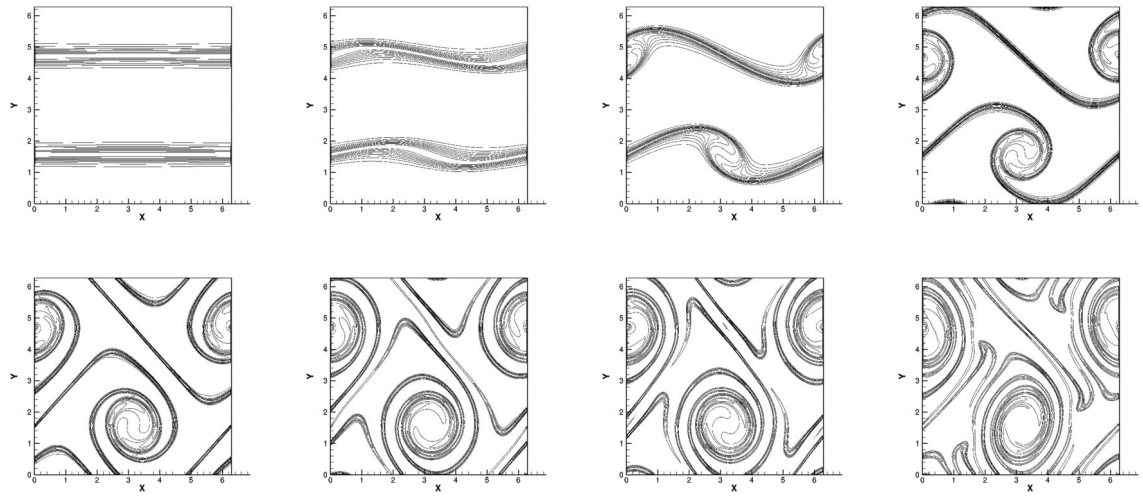

Figure 5. Evolution of Double Shear Layer

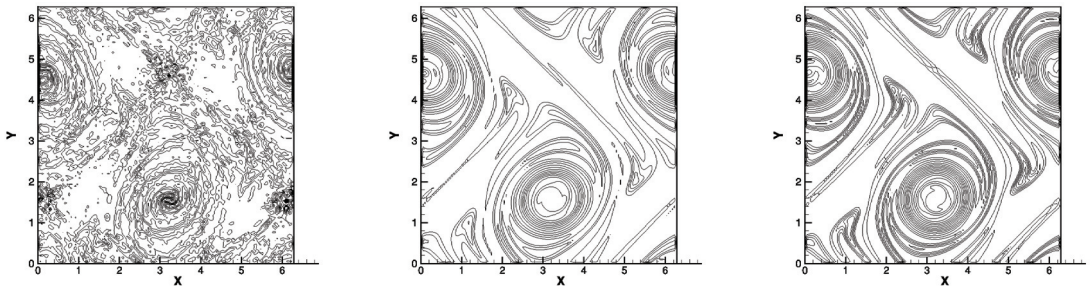

(a) 2nd order central (b) 5th order WENO (conservative) (c) 5th order (non-conservative)

Figure 6. Comparison of schemes - Double Shear Layer

distribution given by[16]

$$\omega(x, y, z) = \omega_0 \exp[-(\frac{r}{a})^2] \tag{11}$$

where $r = [(x - x_c)^2 + (y - y_c)^2 + z^2]^{\frac{1}{2}}$ is the radial distance from the center of the cross-section. The domain is a cube of length 2π. The cross-section of each ring is centered at $x_c = X_c + R\cos\theta$, $y_c = Y_c + R\sin\theta$ where X_c, Y_c are the coordinates of the center of the vortex ring lying in the $z = 0$ plane. R is the radius of the vortex ring, θ is the azimuthal angle in the x-y plane and a is the thickness of the ring. The rings are centered at $(\pm\frac{1}{2}D\cos\frac{\pi}{4}, \pm\frac{1}{2}D\sin\frac{\pi}{4})$ resulting in a separation distance of D between their centers. In the present study, the values for these parameters are $D = 1.83$, $R = 0.491$, $a = 0.196$ and $\omega_0 = 23.8$.[16] Figure 7 shows the time evolution of the vortex rings interaction for a circulation based Reynolds number of 577 ($Re = \pi\omega_0 a^2/\nu$) (the normalized vorticity magnitude iso-surfaces are plotted). The domain is discretized by a $128 \times 128 \times 128$ grid. The results shown are obtained using fifth order upwind scheme and RK3 time stepping. Similar results are obtained using second order central scheme with AB2 time stepping. These are in good agreement with those in literature.[16,17]

III.E. Coaxial Vortex Ring Leapfrogging

The mutual leapfrogging of two vortex rings with the same sense of rotation is simulated in this problem.[18] As the two vortex rings translate, the leading vortex ring enlarges while the trailing ring shrinks and slips through. This pattern repeats, resulting in an indefinite leapfrogging in the absence of viscosity. In the presence of dissipation, numerical or physical, the vortex rings mutually interact to eventually coalesce into

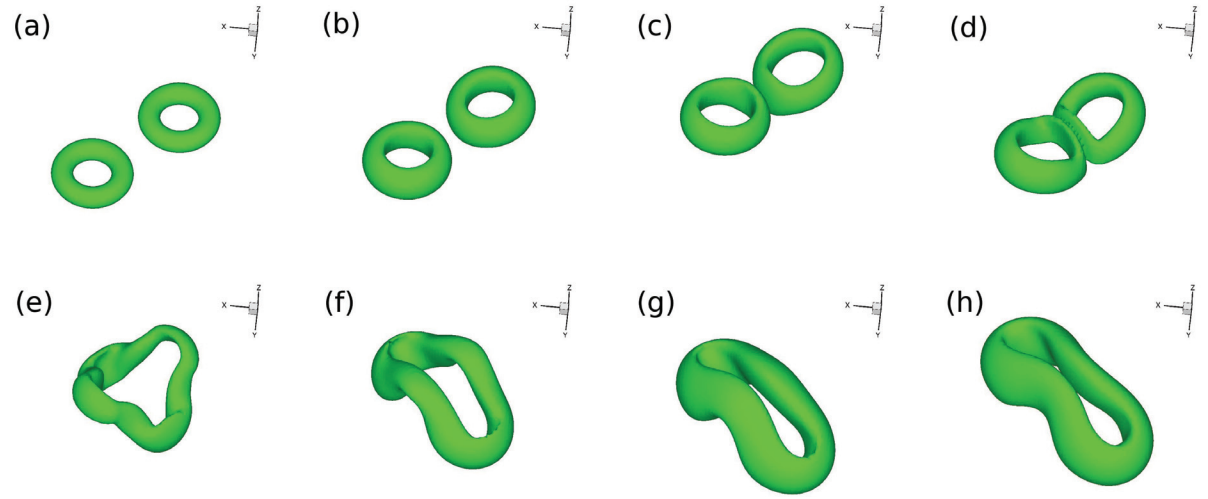

Figure 7. Interaction of Coplanar Vortex Rings

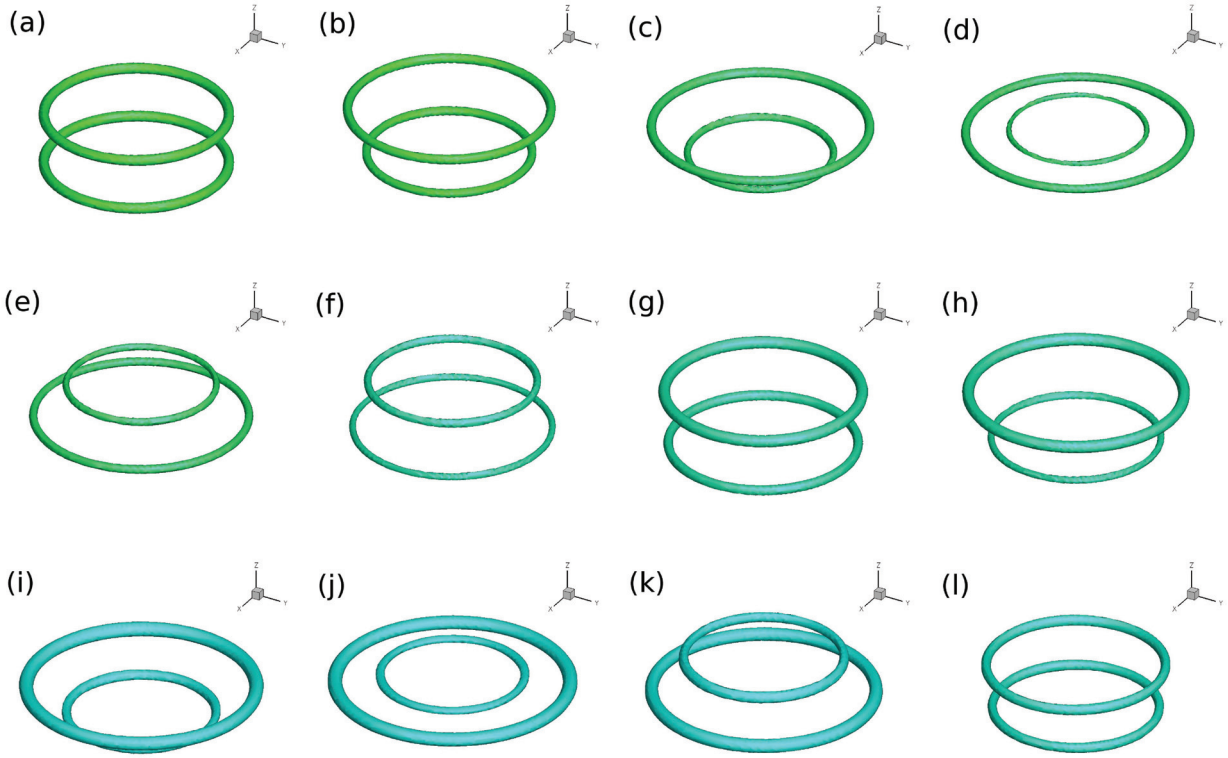

Figure 8. Leapfrogging of coaxial vortex rings

one ring. The thickness of the rings with respect to their radius determines the extent of time during which they leapfrog before coalescing. Large, thin rings leapfrog for a longer duration than small, thick ones.

The problem is solved on a $144 \times 144 \times 144$ grid with periodic boundary conditions on all boundaries. The flow is initialized as two coaxial rings with a Gaussian azimuthal vorticity distribution given by Eq. (11). The circulation $\pi\omega_0 a^2$ is 1 and the ring thickness a/R is 0.05, where R is the ring radius. The initial separation between the rings is $0.6R$. The domain is a cube of length $5R$ in each dimension. The problem is run until

a non-dimensional time of 10 (for $R = 1$) allowing two complete cycles of the rings leapfrogging around each other. The fifth order upwind WENO scheme is used with RK3 time stepping. Both the conservative and non-conservative flux formulations are used and there are no perceptible differences in the solution. Figure 8 shows vorticity magnitude iso-surfaces for one complete cycle of the leapfrogging motion. While the leapfrogging motion is captured by the algorithm, there is a gradual weakening of the vortex strengths due to numerical dissipation. The results demonstrate the ability of the solver to handle inviscid flows with sharp gradients (concentrated vortices) and accurately capture the flow features.

IV. Summary

A high order algorithm is developed based on a conservative, upwind flux reconstruction to simulate high Reynolds number flows. The algorithm is validated over benchmark incompressible flow problems. The numerical errors and convergence behavior are studied for various orders and flux formulations on the isolated vortex convection problem for which the exact solution is available. It is observed that the non-conservative flux formulation results in solutions with less dissipation. Second order convergence is observed in all cases although higher order spatial reconstruction is used. The Poisson step is thought to be a limiting factor for the algorithm. The performance of the algorithm is also demonstrated for inviscid problems. The inviscid shear layer test is simulated which involves strong gradients and non-oscillatory results are obtained using the high order upwind flux reconstruction. The inviscid leapfrogging of coaxial vortex rings is simulated to demonstrate the performance of the algorithm for problems with small regions of concentrated vorticity. Overall, satisfactory results are obtained for both viscous and inviscid problems.

References

[1]Temam, R., "Navier Stokes Equations", North-Holland, Amsterdam, 1977

[2]Quartapelle, L., "Numerical Solutions of the Incompressible Navier-Stokes Equations", International Series of Numerical Mathematics, Vol. 113, Birkhauser-Verlag, Basel, 1993

[3]Rempfer D., "On Boundary Conditions for Incompressible Navier-Stokes Problems", *Applied Mechanics Reviews*, Vol. 59, 2006

[4]Ferziger, J.H., Perric, M., "Computational Methods for Fluid Dynamics" (3^{rd} Ed.), Springer, New York, 2002

[5]Chung, T.J., "Computational Fluid Dynamics", Cambridge University Press, Cambridge, 2002

[6]Chorin, A.J., "A Numerical Method for Solving Incompressible Viscous Flow Problems", *Journal of Computational Physics*, Vol. 2, No. 1, 1967, pp. 12-26

[7]Chorin, A.J., "Numerical Solution of the Navier Stokes Equations", *Mathematics of Computation*, Vol. 22, No. 104, 1968, pp. 745-762

[8]Chorin, A.J., "On the Convergence of Discrete Approximation to the Navier-Stokes Equations", *Mathematics of Computation*, Vol. 23, No. 106, 1969, pp. 341-353

[9]Steger, J.L., Kutler P., "Implicit Finite-Difference Procedures for the Computation of Vortex Wakes", *AIAA Journal*, Vol. 15, No. 4, 1977, pp. 581-590

[10]Kim, J., Moin, P., "Application of a Fractional Step Method to Incompressible Navier-Stokes Equations", *Journal of Computational Physics*, Vol. 59, No. 2, 1985, pp. 308-323

[11]Zhang J., Jackson T.L., "A high-order incompressible flow solver with WENO", *Journal of Computational Physics*, Vol. 228, 2009

[12]Shu, C.W., Osher S., "Essentially Non-Oscillatory and Weighted Essentially Non-Oscillatory Schemes for Hyperbolic Conservation Laws", ICASE report 1997-65, 1995

[13]Zedan, M., Scheider G.E., "A Three-Dimensional Modified Strongly Implicit Procedure for Heat Conduction", *AIAA Journal*, Vol. 21, No. 2, 1983, pp. 295-303

[14]Ghia U., Ghia K.N., Shin C.T., "High-Re Solutions for Incompressible Flow using the Navier-Stokes Equations and a Multigrid Method", *Journal of Computational Physics*, Vol. 48, No. 3, 1982, pp. 387-411

[15]Levy D., "A stable semi-discreet central scheme for the two-dimensional incompressible Euler equations", *IMA Journal of Numerical Analysis*, Vol. 25, 2005

[16]Hahn S., Iaccarino G., "Towards Adaptive Vorticity Confinement", *47th AIAA Aerospace Sciences Meeting*, Orlando, FL, 2009

[17]Kida S., Takaoka M., Hussain F., "Collision of Two Vortex Rings", *Journal of Fluid Mechanics*, Vol. 230, 1991

[18]Sommerfield, A., "Mechanics of Deformable Bodies", Lectures of Theoretical Physics Vol. II, Academic Press, New York, 1950